Initial stages of oxygen adsorption on In/Si(111)-4×1

Hyungjoon Shim, Heechul Lim, Younghoon Kim, Sanghan Kim, and Geunseop Lee*
Department of Physics, Inha University, Incheon 402-751, Korea

Hye-Kyoung Kim, Chiho Kim, and Hanchul Kim†
Department of Physics, Sookmyung Women's University, Seoul 140-742, Korea

(Received 16 February 2014; revised manuscript received 19 June 2014; published 16 July 2014)

The In/Si(111)4×1 surface with In wires is a prototypical one-dimensional electron system showing a temperature-induced structural phase transition. While most impurities are known to decrease the transition temperature (T_c), oxygen was reported to increase the T_c. In order to understand the exceptional influence of oxygen, we have examined the initial stages of oxygen adsorption on the surface by scanning tunneling microscopy (STM) and density-functional theory (DFT) calculations. Oxygen molecules were found to dissociate and adsorb as atoms on the surface. STM revealed three distinct O adsorption features as well as occasional transformations from one to another. The high-resolution images showed that all three adsorbed O features were located at the center of the In trimer at both edges of the In wire. This registry is in contradiction with the previous theoretical predictions [S. Wippermann *et al.*, Phys. Rev. Lett. **100**, 106802 (2008)]. The present DFT calculations identified two of the features as O atoms incorporated in the *interstitial* region between the In wire and subsurface Si layer.

DOI: 10.1103/PhysRevB.90.035420 PACS number(s): 68.37.Ef, 68.43.Fg, 68.43.Bc

I. INTRODUCTION

The phase transitions in solids have been a subject of fundamental research in both fields of statistical physics and condensed matter physics. Recently, the phase transitions in reduced-dimensional systems have attracted renewed interest since both structural and electronic transitions were reported in a number of metal-induced superstructures formed on the surfaces [1–9]. The nature of the surface phase transition and the influence of defects and impurities on the phase transition have been the focus of intensive research in these reduced-dimensional systems.

The In/Si(111)-4×1 surface at room temperature (RT) is a low-dimensional system, where its phase transition has been studied extensively [3,10–17]. This surface undergoes a structural phase transition to an 8×2 structure when the temperature is reduced to below 130 K [3,12,13]. A metal-insulator transition was also reported to occur at the same temperature, accompanying the structural phase transition [3,13]. Owing to the (quasi-)one-dimensional nature of this surface, the phase transition was originally interpreted in terms of the charge-density-wave transition [3]. In contrast, other studies proposed a different explanation [18,19].

Global characteristics such as the transition temperature (T_c) and transport property of this In/Si(111)-4×1 surface have been reported to be affected significantly by small amounts of defects [13,20–28]. In a recent series of diffraction experiments, the defects created by depositing metal atoms (In and Na) or by exposing the surface to gases (hydrogen and oxygen) were found to change the transition temperature [23–25,27]. Of particular interest was the adsorption of oxygen, which increased the T_c of the phase transition of the In/Si(111)-4×1 surface, whereas the other defects reduced it. The effect of oxygen defects increasing T_c is unique and extraordinary [24]. Two possibilities have been suggested to explain the O-induced increase in T_c; hole doping or a correlated arrangement of the O-induced defects. The former possibility was based on the property of oxygen taking electrons from the surface upon adsorption. A theoretical calculation, however, indicated that both electron and hole doping reduced T_c [29]. A recent angle-resolved photoelectron spectroscopy study found that the oxygen adsorption increases the band filling of the one-dimensional surface metallic bands, which is in contrast to the expected hole doping [30]. Therefore the hole doping effect of oxygen adsorption is unlikely to account for the increase in T_c. On the other hand, the latter possibility, correlated arrangement of the O-induced defects, requires further an atomic-level investigations.

Knowledge of the local properties, such as the identities of the adsorbed species and adsorption sites are essential to understanding both the local structural changes and the role of defects in the phase transition. While the adsorption site and local perturbation of the atomic H have been determined by scanning tunneling microscopy (STM) and first-principles theoretical calculations [22], little is known regarding the adsorption of oxygen. In a previous STM study, dark features were observed after exposing the surface to the oxygen gas and interpreted as vacancies due to surface etching [22]. Recently, a theoretical study considered the adsorption of atomic oxygen and predicted its adsorption site as well as its influence on surface conductance [31].

In the present study, the adsorption of oxygen on the In/Si(111)-4×1 surface in the initial stages was examined by STM and first-principles calculations. Experimentally, three distinct O adsorption features were observed in the STM images after exposing the surface at RT. All these adsorbed features were attributed to the atomic O adsorbed dissociatively from the molecules. Density-functional theory calculations identified two of the features: O atoms incorporated in the interstitial region between the In wire and Si substrate. The third adsorption feature remains to be identified.

*glee@inha.ac.kr
†hanchul@sookmyung.ac.kr

 ©2014 American Physical Society

II. EXPERIMENT

The STM experiments were performed in an ultrahigh vacuum chamber with a base pressure below 1.0×10^{-10} Torr. The In/Si(111)-4×1 surface was prepared by the deposition of 1 ML of In from a Ta-wrapped In source onto a clean Si(111) surface at approximately 700–750 K [32]. The formation of the In/Si(111)-4×1 surface was confirmed by STM scanned at RT. Oxygen gas was introduced into the chamber through a variable leak valve during scanning. This ensured that the initial adsorption of oxygen as various adsorption features could be identified with certainty. The partial pressure of the O_2 gas, which back-filled the chamber was maintained at 2×10^{-9}–1×10^{-8} Torr. The amount of oxygen gas introduced in the chamber was controlled by the continued time during scanning at a fixed pressure and is given in units of L (1 L = 1×10^{-6} Torr sec) for a relative comparison.

III. RESULTS

Figure 1(a) presents STM images of the In/Si(111)-4×1 surface exposed to 4.7 L of O_2 gas in total (1×10^{-9} Torr, 4700 s). These images were taken at a negative sample bias ($V_s = -1.0$ V), representing the spacial distribution of the occupied surface electronic states. Two types of adsorption features, one bright (B) and the other dark (D), were clearly distinguishable. Both were attributed unambiguously to the oxygen adsorption features, because they appeared newly in the images [see Figs. 1(b)–1(d)] taken successively over time during the O_2 dosing. These adsorption features occasionally transform to each other, as shown in Figs. 1(b)–1(d).

Both the B and D adsorption features increased in number as the exposure to O_2 proceeded, indicating that they were certainly related to oxygen adsorption. They occupied either side of the In chain and showed a preference for one side over the other. A comparison with a Si(111)-7×7 surface showed that the preferential occupation side corresponds to the side of the unfaulted half unit of the 7×7 cell, i.e., $\langle 11\bar{2}\rangle$ side. This preference in the adsorption side is the same as that of the adsorption of H atoms [22]. By counting the adsorption features altogether, the ratio between the major and minor adsorption sides was approximately 2:1. This preference indicates the influence of the subsurface layer on the adsorption, which is not symmetrical under the reflection with respect to the centerline of the In chain. The apparent glide plane symmetry of the In wires is absent in the Si(111) substrate.

Although the dark features in Fig. 1 appear similar, they are divided into two different types, D_1 and D_2. This is clearly shown in Fig. 2, where the filled- and the empty-state images of the same area are compared. The D_1 and D_2 oxygen features, both appearing dark in the filled state, were clearly distinguished in the empty-state image [see Fig. 2(b)]. D_1 appeared as a bright protrusion with two bright satellites (marked with arrowheads) at the opposite side of the chain. In contrast, D_2 appeared dark (depressed than the background). The opposite side of the D_2 feature within the chain also appeared bright but it was not as prominent as the satellites of the D_1 feature.

The oxygen can be adsorbed on the surface both in the atomic (O) and molecular (O_2) forms. Determining unambiguously whether the adsorbed oxygen is an atom or a molecule is quite difficult. However, it has been well known that oxygen molecules are dissociated and adsorbed as atoms on metal surfaces at RT [33,34]. Adsorption of molecular oxygen in physisorbed or chemisorbed form has been observed only when the temperature was significantly reduced [35,36]. In our case, a good agreement between the experimental adsorption features with the calculated atomic oxygen species (as it will be shown later) validates the adsorption of oxygen as atoms on the In/Si(111)-4×1 surface at RT. Therefore we rule out the possibility of the observed STM features as O_2 molecules.

Information on the adsorption sites of the atomic O can be obtained from the high-resolution images compared with the atomic structure model, as shown in Fig. 3. In the STM images of the clean surface with low-bias voltages ($|V_s| < 0.5$ V) [Fig. 3(a)], bright protrusions form zigzag chains. Each bright protrusion coincides with the center of a triangle formed by one inner-row In atom and two outer-row (edge-row) In atoms [solid circle in Figs. 3(a) and 3(b)]. In Figs. 3(c)–3(e), which show STM images ($V_s = +0.36$ V) of the O-adsorbed surface, all three oxygen features are located on the tops of these bright protrusions. The B feature appears much brighter [Fig. 3(c)], D_1 is similar [Fig. 3(d)], and D_2 is slightly darker [Fig. 3(e)] than the surrounding protrusions at this low bias. D_1 and D_2 appear similar in that their protrusions are surrounded by dark depressed area. On the other hand, they are distinguishable by the relative brightness of the central protrusions, i.e., D_2 is darker than D_1. In the vicinity of these defects, ×2 modulations are developed and decay with the distance along the row from the defects. These O-defect-induced ×2 modulations are

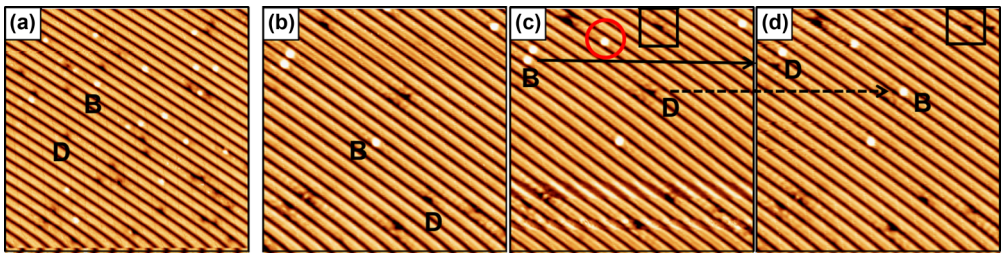

FIG. 1. (Color online) (a) Representative STM image of the In/Si(111)-4×1 surface exposed to O_2 gas (4.7 L) at RT. Two types of adsorption features, bright (B) and dark (D), are clearly visible. (b)–(d) STM images taken successively over time at approximately two-minute intervals during the O_2 dosing with 1×10^{-9} Torr. During dosing, new adsorption features appeared [B (circle) and D (rectangle)] and the transformation between the adsorption features [B-to-D (solid arrow) and D-to-B (dashed arrow)] were observed. The images were filled-state images taken at $V_s = -1.0$ V.

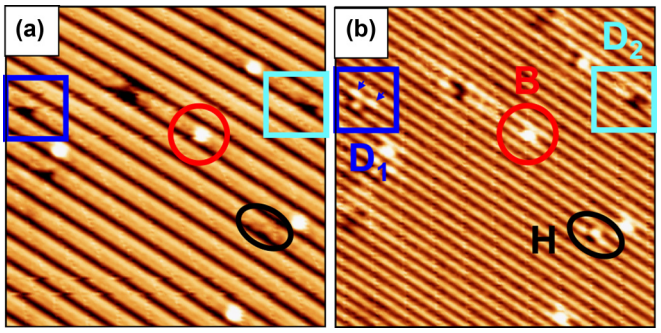

FIG. 2. (Color online) STM images taken with opposite-polarity bias voltages over the same area: (a) filled state ($V_s = -1.0$ V) and (b) empty state ($V_s = +1.0$ V). The three distinct features are labeled as B, D_1, and D_2. One atomic H adsorption feature (cracked from residual gas by ion gauge filament) was also observed (ellipse). The atomic H feature was distinguished from the bright oxygen feature B by its a distinct "seagull" shape with two side lobes in the empty-state image (see Ref. [22]).

similar to that observed for atomic H adsorption [22]. This confirms that the defects on the 4×1 surface induce common ×2 modulations even at RT, which are inherently different from the ×2 structure in the 8×2-LT phase.

The experimentally determined adsorption locations for all three O adsorption features clearly contrast with the prediction of the O adsorption site in the previous theoretical study [31]. Wippermann *et al.* reported that the minimum energy position of the adsorbed atomic O is a threefold-coordinated site (marked as × in Fig. 3) at the center of a triangle formed by two inner-row In atoms and one outer-row In atom. In

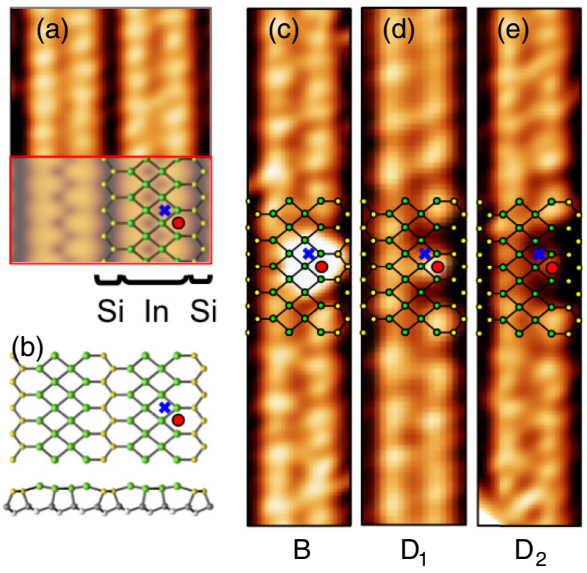

FIG. 3. (Color online) (a) Experimental (top) and simulated (bottom) STM images at $V_s = +0.2$ V, and (b) atomic structure of the clean In/Si(111)-4×1 surface. (c)–(e) High-resolution STM images ($V_s = +0.2$ V) of the three O adsorption features, B, D_1, and D_2. The O adsorption sites are indicated by solid circles (•). A theoretical adsorption site from the previous study (Ref. [31]) is also indicated (×) for comparison.

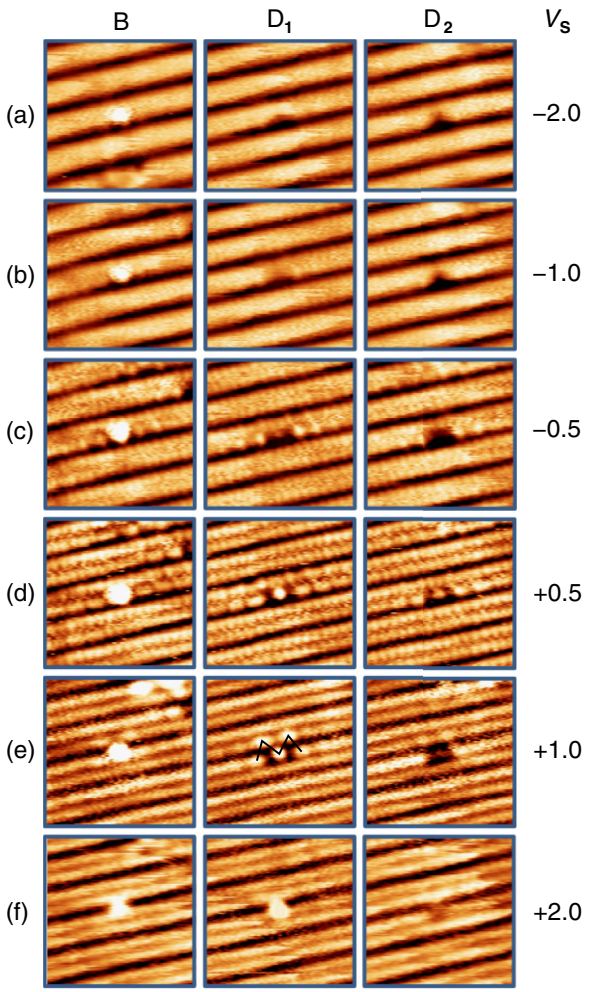

FIG. 4. (Color online) Bias dependence of the appearances of the O-induced STM features (B, D_1, and D_2) on the preferred side in the STM images. The sample bias voltages representing for the filled ($V_s < 0$) and empty ($V_s > 0$) states are given.

the low-bias voltage STM images, the predicted O adsorption site falls in-between (not on top of) the protrusions along the chain as indicated by × in Fig. 3(b). Therefore there is a clear discrepancy between the previous theoretical adsorption site and the sites determined by these experimental observations.

Figure 4 shows the bias-dependent appearances in the STM images of these three O-adsorption features in the preferred side. The B feature appears bright over the whole bias-voltage range between −2.0 and +2.0 V. In contrast, the D features (D_1 and D_2) show nontrivial bias-dependent variations in the STM images. The bias-voltage regimes for the appearance variation can be divided into three. In the filled-state regime (-2.0 V $< V_s < -0.2$ V), both the D_1 and D_2 features are dark and barely distinguishable. In the low-bias empty-state regime ($+0.2$ V $< V_s \leqslant +0.5$ V), the two D features appear similar, showing a localized central ball-like protrusion with neighboring satellite protrusions. The main difference between the D_1 and D_2 features in this bias regime is the relative brightness of the central ball features, D_1 being brighter than D_2. Other than this brightness difference, it is difficult to distinguish between the D_1 and D_2 features.

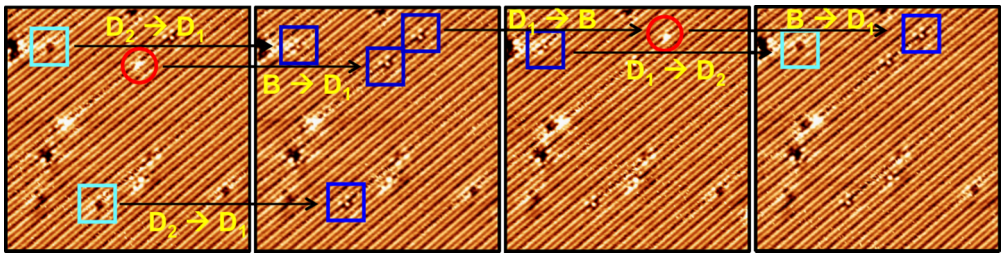

FIG. 5. (Color online) Series of STM images ($V_s = +1.24$ V) taken successively with time over the same area, showing the mutual transformations between the O-induced adsorption features. The B-to-D_1, D_1-to-B, D_1-to-D_2, and D_2-to-D_1 transformations are indicated by the arrows.

As the empty-state bias-voltage increases ($V_s > +0.5$ V), the D_1 and D_2 features show contrasting changes in brightness. The central ball feature of the D_1 becomes continuously brighter as the voltage is increased. The feature become as bright as the B feature at $V_s \geqslant +1.7$ V so that it is barely discernible from the B feature [see Fig. 4(f)]. In contrast, the central ball feature of the D_2 became dark as the bias-voltage was increased, making the D_2 easily distinguishable from the D_1 feature. We note that the bias voltages between +0.8 and +1.3 V were most suitable for distinguishing the three O adsorption features without ambiguity. In particular, the central ball-like protrusion of the D_1 feature with a four neighboring satellite protrusions forms a distinct M-shaped appearance [see the central panel of Fig. 4(e)]. This makes the D_1 feature easily distinguishable from the other adsorption features. Identification of the adsorption features at these bias voltages is important because they occasionally transform to each other over time, as shown in Figs. 1(c) and 1(d).

Figure 5 presents a series of STM images taken consecutively over the same area. The time interval between the successive images was approximately two minutes. The transformations between the adsorption features, B-to-D_1, D_1-to-B, D_1-to-D_2, and D_2-to-D_1, are indicated by arrows. The mutual transformations between the B and D_1 features were observed most frequently with at an almost equal rate. In comparison, transformations between the D_1 and D_2 features were observed much less frequently, at one tenth the rate, compared to the transformations between the B and D_1 features. Interestingly, the D_1-to-D_2 change was less frequent than the reversed change. The transformations between B and D_2 were also observed but they were quite rare. The oxygen was adsorbed mostly as the B and D_2 features in the initial stage of adsorption. In contrast, the D_1 features were formed mostly by the transformation from the other adsorption features, and its population grew as a result of the unbalanced transformation ratios. A quantitative determination of the definite relative ratio of the transformations, however, was not attempted because several different sample surfaces showed a range of statistics.

Educated by the experimental results, we have performed *ab initio* pseudopotential calculations based on density-functional theory (DFT) within the local density approximation (LDA) [37]. A kinetic energy cutoff of 400 eV and a theoretical lattice constant of 5.39 Å were used. A 4×2 ***k***-point mesh in the surface Brillouin zone of the 4×9 surface supercell (which is equivalent to a 4×18 ***k***-point mesh in the 4×1 Brillouin zone) was used to perform the momentum-space integration, and the ultrasoft pseudopotentials were used to describe the electron-ion interaction [38]. The room-temperature 4×1 In nanowire system was modeled by a repeated slab comprised of top surface 4×1 In wires and Si Seiwatz chains, the three-bilayer Si substrate, and the bottom H layer passivating the dangling bonds of the Si substrate. The repeated slabs were intervened by a 19-Å-thick vacuum region. All the atoms, other than those in the two bottom Si and H layers, were relaxed until the atomic forces were less than 0.001 eV/Å.

Six distinct sites (a–f) were investigated to determine the stable configurations for an adsorbed O atom, as shown in Fig. 6(a). Table I lists the resulting adsorption energies, defined as

$$E_{\rm ad} = E_{\rm DFT}(\text{clean surface}) + E_{\rm DFT}(\text{O atom}) - E_{\rm DFT}(\text{O adsorbed surface}).$$

On the surface, the f site (S_f) was the most stable, among all the six sites, followed by the a site (S_a). This is in agreement with the experimental observation that the O-induced STM features are located at the outer triangle (solid circle in Fig. 3), which is in contradiction to the prediction of an inner triangle site (the b and e sites, also × in Fig. 3) from previous DFT calculations [31]. We have examined the convergence of the adsorption energies with respect to the simulation cell by varying the supercell size from 4×3 to 4×9, and found that the relative stability of different configurations did not change.

More strikingly, an O atom becomes further stabilized if incorporated into the interstitial region between the In wire and Si substrate. The interstitial sites below a and f were approximately 0.4 eV more stable than the corresponding surface adsorption sites. On the other hand, other interstitial locations below the b–e sites were either less stable than the surface or unstable. In the interstitial region below the a (f) site, there were two distinct stable configurations, I_{a1} and I_{a2} (I_{f1} and I_{f2}), as shown in Table I. The interstitial configurations below the f site were more stable than those below the a site. This is consistent with the experimental observation that the preferred O adsorption sites are in the unfaulted half-unit-cell direction of Si(111)-7×7. From now on, we will focus on the preferred (major) adsorption sites.

In both interstitial structures, I_{f1} [Fig. 6(b)] and I_{f2} [Fig. 6(c)], the incorporated O atom forms bonds with three adjacent In atoms in the outer triangle and an underlying Si atom on the substrate. Although the O atom is located at a similar position and has the same coordination number in

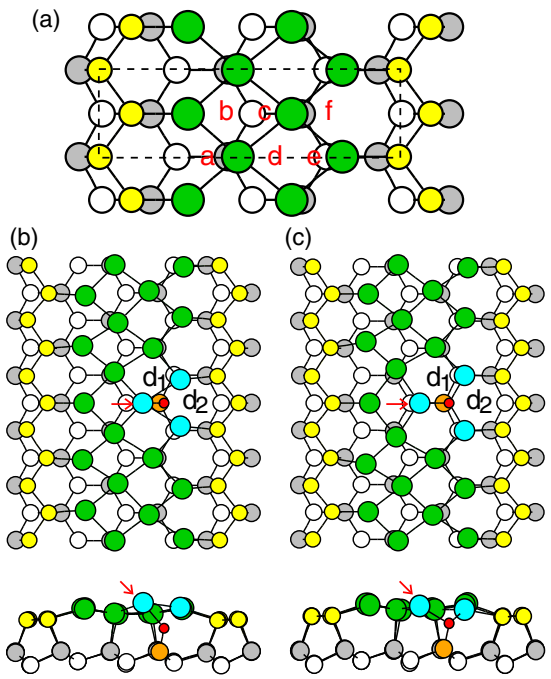

FIG. 6. (Color online) (a) Pristine In/Si(111)-4×1 surface with six different adsorption sites marked by a–f. The 4×1 surface unit cell is denoted by a dashed rectangle. (b) and (c) Two low-energy interstitial O structures below the f site: (b) I_{f1} and (c) I_{f2}. The green and cyan circles are unreacted and reacted In atoms, respectively. The Seiwatz Si atoms are represented by yellow circles, and the substrate Si atoms denoted by grey and white circles. The substrate Si atom that reacted with O is denoted by the orange circle. The arrows indicate the reacted In atom, which shows a characteristic structural difference between I_{f1} and I_{f2} (see the text).

both configurations, the reacted In atoms show significantly different structural features. In I_{f1}, the reacted inner In atom [indicated by an arrow in Fig. 6(b)] is lifted upward, resulting in an *out-of-plane* displacement, whereas the corresponding In atom [indicated by an arrow in Fig. 6(c)] in I_{f2} shows a significant *in-plane* displacement away from the O atom. As

TABLE I. Adsorption energy (E_{ad}) of an O atom on the In/Si(111)-4×1 surface referred to an isolated O atom and the pristine In/Si(111)-4×1 surface. Adsorption energies in parentheses are obtained using a 4×3 surface supercell. The adsorption sites are designated in Fig. 6(a).

	Adsorption site	E_{ad} (eV/O atom)
Surface	S_a	6.75 (6.71)
	S_b	6.37 (6.22)
	S_c	6.57 (6.51)
	S_d	6.60 (6.54)
	S_e	6.45 (6.29)
	S_f	6.79 (6.74)
Interstitial	I_{a1}	7.18
	I_{a2}	7.12
	I_{f1}	7.24
	I_{f2}	7.20

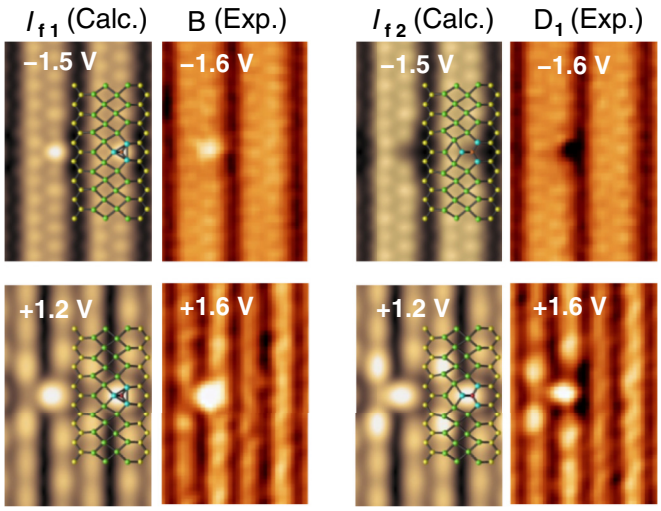

FIG. 7. (Color online) Simulated STM images of the two low-energy structures, I_{f1} and I_{f2}, compared to the experimental features, B and D_1. (Left) I_{f1} vs the B feature. (Right) I_{f2} vs the D_1 feature [40].

a consequence, the outer triangle formed by the three reacted In atoms became smaller in I_{f1} with interatomic distances ($d_1 = 3.07$ Å and $d_2 = 3.23$ Å), but became larger in I_{f2} with interatomic distances ($d_1 = 3.68$ Å and $d_2 = 3.87$ Å), compared to the pristine case, where the corresponding interatomic distances are 2.95 and 3.81 Å. Due to the bond formation with the more electronegative O atom, the three reacted In atoms are expected to lose electrons compared with unreacted In atoms. Considering the fact that the bright protrusions in the filled-state STM images are contributed by the outer In triangles [22], the electron deficiency at three reacted In atoms would lead to a diminished protrusion, i.e., a dark depression. However, such an electronic contribution will compete with a geometric contribution of the reacted inner In atom.

Constant-current STM images were simulated for the two stable interstitial adsorption structures, I_{f1} and I_{f2}, by varying the bias voltage in both filled- and empty-states employing the Tersoff-Hamann approximation [39]. Figure 7 compares the simulated STM images with the experimental images. For I_{f1}, a bright protrusion appeared at the O site in the filled- and the empty-state simulations, as shown in the left panel of Fig. 7, which is of a geometric origin due to the upward relaxed inner In atom. In addition, neighboring bright satellite features were also visible in the empty-state image. These simulated STM images of I_{f1} were well compared with the experimental O-induced B feature, as shown in Fig. 7.

In the case of I_{f2} in the right panel of Fig. 7, the electronic origin (*electron deficiency* at the three reacted In atoms) manifests in the filled state and the O adsorption site appears as a *dark depression*. On the other hand, the filled-state dark depression turns into a bright protrusion in the empty state, which is in agreement with the O-induced D_1 feature of the experimental STM images. In addition, the four bright satellite features were slightly more prominent in I_{f2} than in I_{f1}. The simulated STM images were examined for other locally stable configurations in Table I, but no O-induced structure that reproduces the bias-dependence of the experimental D_2 feature could be identified (see the right-most column in Fig. 4)

Consequently, both the experimental B and D_1 features at the majority side (right subchain in Fig. 6) are identified as I_{f1} and I_{f2}, respectively. Based on the slight change in the O location in both configurations, the transition barrier between I_{f1} and I_{f2} was expected to be small, which is comparable to the experimental observation that a mutual transformation between the B and D_1 features occurs frequently [41].

Now that we identified two O-induced structures, it is worthwhile to comment on their implication to the peculiar T_c-increasing effect of O defects. A $\times 2$ modulation was observed near the O defects, but it differs from the 8×2-LT structure. Thus our RT study hardly provides insights on the mechanism of the T_c increase by oxygen adsorption. However, we speculate that the local structural distortions around O defects may change at lower temperature, facilitating the formation of the 8×2-LT phase. Further microscopic study at variable temperatures, near the transition in particular, is needed to investigate such a possibility

IV. SUMMARY AND CONCLUSION

The adsorption of oxygen on the In/Si(111)-4×1 surface in the initial stages was examined by STM and first-principles calculations. Three distinct oxygen adsorption features were observed in the STM images and attributed to the atomic O dissociatively adsorbed from the O_2 molecules. The transformations among the three O adsorption features were observed occasionally. Based on the energetics and STM image simulations calculated by density-functional theory, two of the features were identified as an O atom incorporated in the interstitial region between the In wire and Si subsurface layer. On the other hand, the third O adsorption feature in the experiment was not consistent with any of the locally stable adsorption structures considered in the calculations. Therefore more study will be needed to identify this adsorption feature.

ACKNOWLEDGMENTS

G.L. acknowledges the support of Quantum Metamaterials Research Center (R11-2008-053-02001-0) and Basic Science Research Program (No. 2010-0012231) through the National Research Foundation of Korea (NRF) funded by the Ministry of Education, Science and Technology (MEST). H.K. is grateful for the support from the Mid-career Researcher Program (No. 2008-0059595) and EDISON program (No. 2012M3C1A6035304) through NRF funded by MEST. The calculations were supported by the Strategic Supercomputing Support Program from the Korea Institute of Science and Technology Information (No. KSC-2008-S02-0010).

[1] J. M. Carpinelli, H. H. Weitering, E. W. Plummer, and R. Stumpf, Nature (London) **381**, 398 (1996).
[2] H. H. Weitering, J. M. Carpinelli, A. V. Melechko, J. Zhang, M. Bartkowiak, and E. W. Plummer, Science **285**, 2107 (1999).
[3] H. W. Yeom, S. Takeda, E. Rotenberg, I. Matsuda, K. Horikoshi, J. Schaefer, C. M. Lee, S. D. Kevan, T. Ohta, T. Nagao, and S. Hasegawa, Phys. Rev. Lett. **82**, 4898 (1999).
[4] J. R. Ahn, P. G. Kang, K. D. Ryang, and H. W. Yeom, Phys. Rev. Lett. **95**, 196402 (2005).
[5] P. C. Snijders, S. Rogge, and H. H. Weitering, Phys. Rev. Lett. **96**, 076801 (2006).
[6] A. van Houselt, T. Gnielka, J. M. J. Aan van de Brugh, N. Oncel, D. Kockmann, R. Heid, K.-P. Bohnen, B. Poelsema, and H. J. W. Zandvliet, Surf. Sci. **602**, 1731 (2008).
[7] K. Swamy, A. Menzel, R. Beer, and E. Bertel, Phys. Rev. Lett. **86**, 1299 (2001).
[8] T. Nakagawa, G. I. Boishin, H. Fujioka, H. W. Yeom, I. Matsuda, N. Takagi, M. Nishijima, and T. Aruga, Phys. Rev. Lett. **86**, 854 (2001).
[9] J. Martínez-Blanco, V. Joco, H. Ascolani, A. Tejeda, C. Quiros, G. Panaccione, T. Balasubramanian, P. Segovia, and E. G. Michel, Phys. Rev. B **72**, 041401 (2005).
[10] C. Kumpf, O. Bunk, J. H. Zeysing, Y. Su, M. Nielsen, R. L. Johnson, R. Feidenhans'l, and K. Bechgaard, Phys. Rev. Lett. **85**, 4916 (2000).
[11] K. Sakamoto, H. Ashima, H. W. Yeom, and W. Uchida, Phys. Rev. B **62**, 9923 (2000).
[12] T. Uchihashi and U. Ramsperger, Appl. Phys. Lett. **80**, 4169 (2002).
[13] T. Tanikawa, I. Matsuda, T. Kanagawa, and S. Hasegawa, Phys. Rev. Lett. **93**, 016801 (2004).
[14] S. J. Park, H. W. Yeom, S. H. Min, D. H. Park, and I.-W. Lyo, Phys. Rev. Lett. **93**, 106402 (2004).
[15] G. Lee, J. Guo, and E. W. Plummer, Phys. Rev. Lett. **95**, 116103 (2005).
[16] J. Guo, G. Lee, and E. W. Plummer, Phys. Rev. Lett. **95**, 046102 (2005).
[17] S. J. Park, H. W. Yeom, J. R. Ahn, and I.-W. Lyo, Phys. Rev. Lett. **95**, 126102 (2005).
[18] J.-H. Cho, D.-H. Oh, K. S. Kim, and L. Kleinman, Phys. Rev. B **64**, 235302 (2001).
[19] C. González, F. Flores, and J. Ortega, Phys. Rev. Lett. **96**, 136101 (2006).
[20] S. V. Ryjkov, T. Nagao, V. G. Lifshits, and S. Hasegawa, Surf. Sci. **488**, 15 (2001).
[21] S. S. Lee, J. R. Ahn, N. D. Kim, J. H. Min, C. G. Hwang, J. W. Chung, H. W. Yeom, S. V. Ryjkov, and S. Hasegawa, Phys. Rev. Lett. **88**, 196401 (2002).
[22] G. Lee, S.-Y. Yu, H. Kim, and J.-Y. Koo, Phys. Rev. B **70**, 121304 (2004).
[23] H. Shim, S.-Y. Yu, W. Lee, J.-Y. Koo, and G. Lee, Appl. Phys. Lett. **94**, 231901 (2009).
[24] G. Lee, S.-Y. Yu, H. Shim, W. Lee, and J.-Y. Koo, Phys. Rev. B **80**, 075411 (2009).
[25] T. Shibasaki, N. Nagamura, T. Hirahara, H. Okino, S. Yamazaki, W. Lee, H. Shim, R. Hobara, I. Matsuda, G. Lee, and S. Hasegawa, Phys. Rev. B **81**, 035314 (2010).
[26] H. Morikawa, C. C. Hwang, and H. W. Yeom, Phys. Rev. B **81**, 075401 (2010).
[27] W. Lee, H. Shim, and G. Lee, J. Korean Phys. Soc. **56**, 943 (2010).

[28] S. Wall, B. Krenzer, S. Wippermann, S. Sanna, F. Klasing, A. Hanisch-Blicharski, M. Kammler, W. G. Schmidt, and M. Horn-von Hoegen, Phys. Rev. Lett. **109**, 186101 (2012); H. Shim, J. Yeo, G. Lee, and H. Kim, *ibid.* **111**, 149601 (2013); T. Frigge, S. Wall, B. Krenzer, S. Wippermann, S. Sanna, F. Klasing, A. Hanisch-Blicharski, M. Kammler, W. G. Schmidt, and M. Horn-von Hoegen, *ibid.* **111**, 149602 (2013).

[29] W. G. Schmidt, M. Babilon, C. Thierfelder, S. Sanna, and S. Wippermann, Phys. Rev. B **84**, 115416 (2011).

[30] S. H. Uhm and H. W. Yeom, Phys. Rev. B **88**, 165419 (2013).

[31] S. Wippermann, N. Koch, and W. G. Schmidt, Phys. Rev. Lett. **100**, 106802 (2008).

[32] G. Lee, S.-Y. Yu, H. Kim, J.-Y. Koo, H.-I. Lee, and D. W. Moon, Phys. Rev. B **67**, 035327 (2003).

[33] F. Besenbacher and J. K. Nrskov, Prog. Sur. Sci. **44**, 5 (1993).

[34] J. Wintterlin, R. Schuster, and G. Ertl, Phys. Rev. Lett. **77**, 123 (1996).

[35] T. Zambelli, J. V. Varth, J. Wintterlin, and G. Ertl, Nature (London) **390**, 495 (1997).

[36] X.-G. Wang and G. B. Fisher, Phys. Rev. Lett. **99**, 066101 (2007).

[37] G. Kresse and J. Furthmüller, Phys. Rev. B **54**, 11169 (1996).

[38] D. Vanderbilt, Phys. Rev. B **32**, 8412 (1985).

[39] J. Tersoff and D. R. Hamann, Phys. Rev. Lett. **50**, 1998 (1983).

[40] Since DFT calculations tend to underestimate the empty-state eigenvalues, a simulated empty-state image is to be compared with a higher-bias experimental one.

[41] The possibility to associate the unidentified D_2 feature with a molecular adsorption of O_2 is excluded in that the mutual transformations among the three features from one to another were observed for the *isolated* ones. Such observations indicate that all the three features have the same origin, i.e., O atoms.